Chapter 6

A robust adaptive numerical method for nonlinear singularly perturbed Volterra integro-differential equations

We consider following singularly perturbed nonlinear Volterra integro-differential equation (VIDE)

$$\begin{cases} \mathcal{T}y := \varepsilon y' + f(x, y(x)) + \displaystyle\int_0^x R(x, s, y(s))\, ds = 0, \quad x \in G = (0, 1], \\ y(0) = B, \end{cases} \tag{6.1}$$

where B is a given constant and $0 < \varepsilon \leq 1$ is a perturbation parameter which in general takes small values. The functions f and R are considered to be sufficiently smooth in $\bar{G} \times \mathbb{R}$ and $\bar{G} \times \bar{G} \times \mathbb{R}$, respectively. Moreover, there exists an $\alpha > 0$ such that $\frac{\partial f}{\partial y} \geq \alpha$ in $\bar{G} \times \mathbb{R}$.

To the best of our knowledge, no published article derived a posteriori error estimate for nonlinear singularly perturbed VIDEs, that is the motivation of this chapter. We discretize problem (6.1) by an implicit finite difference scheme on an arbitrary non-uniform mesh. The scheme comprises of an implicit difference operator for the derivative term and an appropriate quadrature rule for the integral term. We derive a posteriori error estimate in the maximum norm, which can be used with any adaptive moving mesh procedure. We used a variant of de Boor algorithm [54, 115] for this purpose. Numerical experiments are performed and results are reported for validation of the theoretical error estimate.

This chapter is organized as follows: The next section, provides the stability result for the continuous problem (6.1). In Section 6.2, a finite difference discretization of problem (6.1) is described. A posteriori error estimate is derived in Section 6.3. In Section 6.4, we provide numerical results for validation of the theoretical error estimate. Finally, some conclusions are given in Section 6.5.

6.1 Stability of the continuous problem

This section provides the stability result for the continuous problem (6.1). It is used later in a posteriori error analysis of the present numerical scheme for problem (6.1).

Lemma 6.1.1. The solution y of (6.1) satisfies the following stability estimate

$$\|y\|_{\bar{G}} \leq (|B| + \alpha^{-1}\|F\|_G), \quad \text{where} \quad F(x) = -f(x,0) - \int_0^x R(x,s,0)\,ds. \tag{6.2}$$

Further, if y_1 and y_2 are any two functions such that $y_1(0) = y_2(0)$ and

$$\mathcal{T}y_1 - \mathcal{T}y_2 = T,$$

where T is a bounded piecewise continuous function. Then

$$\|y_1 - y_2\|_{\bar{G}} \leq C\|\mathcal{T}y_1 - \mathcal{T}y_2\|_G. \tag{6.3}$$

Proof. We rewrite problem (6.1) as follows

$$\begin{cases} \widetilde{\mathcal{T}}y := \varepsilon y' + r(x)y(x) + \displaystyle\int_0^x K(x,s)y(s)\,ds = F(x), \quad x \in G = (0,1], \\ y(0) = B, \end{cases} \tag{6.4}$$

where

$$r(x) = \frac{\partial f}{\partial y}(x, \tilde{y}(x)),$$

$$K(x,s) = \frac{\partial R}{\partial y}(x, s, \hat{y}(s)),\ \tilde{y}(x) = \theta y(x),\ \hat{y}(s) = \gamma y(s),\ 0 < \theta, \gamma < 1.$$

Now we can use the arguments in [109] to establish (6.2). For proving (6.3), we note that $\mathcal{T}y_1 - \mathcal{T}y_2 = \widetilde{\mathcal{T}}(y_1 - y_2)$, where $\widetilde{\mathcal{T}}$ is defined by (6.4) with

$$r(x) = \frac{\partial f}{\partial y}(x, \bar{y}(x)), \quad K(x,s) = \frac{\partial R}{\partial y}(x, s, \breve{y}(s)),\ \bar{y}(x) = y_2(x) + \theta(y_1(x) - y_2(x)),$$

$$\breve{y}(s) = y_2(s) + \gamma(y_1(s) - y_2(s)),\ 0 < \theta, \gamma < 1.$$

Thus, (6.3) follows using (6.2). □

6.2 The discretization and its stability

We consider an arbitrary non-uniform mesh $G^N = \{0 < x_1 < \cdots < x_N = 1\}$ to discretize G. We define $\bar{G}^N = \{x_0 = 0\} \cup G^N$ and $h_i = x_i - x_{i-1},\ 1 \le i \le N$. Further, we define $D^- V_i := \frac{V_i - V_{i-1}}{h_i}$, for any mesh function V. Now integrating (6.1) over (x_{i-1}, x_i), we get

$$h_i^{-1} \int_{x_{i-1}}^{x_i} \mathcal{T}y \, dx = 0. \tag{6.5}$$

Using (6.1) and the right side rectangle formula we get

$$\varepsilon D^- y(x_i) + f(x_i, y(x_i)) + \int_0^{x_i} R(x_i, s, y(s))\, ds + \mathcal{K}_i^{(1)} + \mathcal{K}_i^{(2)} = 0, \tag{6.6}$$

where

$$\mathcal{K}_i^{(1)} = -h_i^{-1} \int_{x_{i-1}}^{x_i} (\zeta - x_{i-1}) \frac{d}{d\zeta} f(\zeta, y(\zeta))\, d\zeta$$

and

$$\mathcal{K}_i^{(2)} = -h_i^{-1} \int_{x_{i-1}}^{x_i} (\zeta - x_{i-1}) \frac{d}{d\zeta} \left(\int_0^{\zeta} R(\zeta, s, y(s))\, ds \right) d\zeta.$$

We next approximate the integral term by the composite left side rectangle formula

$$\int_0^{x_i} R(x_i, s, y(s))\, ds = \sum_{m=1}^{i} h_m R(x_i, x_{m-1}, y(x_{m-1})) + \mathcal{K}_i^{(3)},$$

where

$$\mathcal{K}_i^{(3)} = \sum_{m=1}^{i} \int_{x_{m-1}}^{x_m} (x_m - \zeta) \frac{d}{d\zeta} R(x_i, \zeta, y(\zeta))\, d\zeta.$$

On combining the approximations we have the relation

$$\varepsilon D^- y(x_i) + f(x_i, y(x_i)) + \sum_{m=1}^{i} h_m R(x_i, x_{m-1}, y(x_{m-1})) + \mathcal{K}_i = 0,\ i = 1, \ldots, N, \quad (6.7)$$

where

$$\begin{aligned} \mathcal{K}_i &= \mathcal{K}_i^{(1)} + \mathcal{K}_i^{(2)} + \mathcal{K}_i^{(3)} \\ &= -h_i^{-1} \int_{x_{i-1}}^{x_i} (\zeta - x_{i-1}) \frac{d}{d\zeta} f(\zeta, y(\zeta))\, d\zeta \\ &\qquad - h_i^{-1} \int_{x_{i-1}}^{x_i} (\zeta - x_{i-1}) \frac{d}{d\zeta} \left(\int_0^{\zeta} R(\zeta, s, y(s))\, ds \right) d\zeta \\ &\qquad + \sum_{m=1}^{i} \int_{x_{m-1}}^{x_m} (x_m - \zeta) \frac{d}{d\zeta} R(x_i, \zeta, y(\zeta))\, d\zeta. \end{aligned} \quad (6.8)$$

Hence, the discretization of problem (6.1) is proposed as follows

$$\begin{cases} \varepsilon D^- Y_i + f(x_i, Y_i) + \sum_{m=1}^{i} h_m R(x_i, x_{m-1}, Y_{m-1}) = 0,\ i = 1, \ldots, N, \\ Y_0 = B. \end{cases} \quad (6.9)$$

Remark 6.2.1. We remark that the authors in [109] used the composite trapezoid rule to approximate the integral term in (6.6). The scheme was proved to be almost

first order accurate on Shishkin meshes. According to us to get almost first order accuracy it is not meaningful to use the composite trapezoid rule. Consequently, we have used the composite left side rectangle formula to approximate the integral term in (6.6). However, one can also use the composite right side rectangle formula to approximate the integral. The discrete problem then will be as follows

$$\begin{cases} \varepsilon D^- Y_i + f(x_i, Y_i) + \sum_{m=1}^{i} h_m R(x_i, x_m, Y_m) = 0, \ i = 1, \ldots, N, \\ Y_0 = B. \end{cases} \tag{6.10}$$

The use of composite right side rectangle formula does not make any difference to the further analysis and numerical results, but the condition $\alpha + h_i \frac{\partial R}{\partial y}(x_i, x_i, \gamma Y_i) \geq \alpha_0 > 0, \ 0 < \gamma < 1$, is required for the proof of stability of the discretization (6.10). A parallel error analysis can be easily done and a similar error estimate can be obtained for scheme (6.10). Therefore, in rest of this chapter we shall be concerned with the numerical scheme (6.9) only.

We next establish that the discrete problem (6.9) is parameter-uniform stable. The following lemma will be used in the proof.

Lemma 6.2.1. Consider the discrete problem

$$\begin{cases} \mathcal{D}^h v_i := \varepsilon D^- v_i + r_i v_i = Q_i, \quad i = 1, \ldots, N, \\ v_0 = B, \end{cases} \tag{6.11}$$

where $r_i \geq \alpha > 0, \ |Q_i| \leq \mathcal{Q}_i$ with $\mathcal{Q}_i$ a non-decreasing function. Then, the solution of (6.11) satisfies

$$|v_i| \leq |B| + \alpha^{-1} \mathcal{Q}_i, \ i = 0, \ldots, N.$$

Proof. It is easy to see that the operator $\mathcal{D}^h$ satisfies the discrete maximum principle. So, considering the mesh function

$$\Psi_i^{\pm} = \pm v_i + |B| + \alpha^{-1}\mathcal{Q}_i,$$

we note that

$$\Psi_0^{\pm} = \pm v_0 + |B| + \alpha^{-1}\mathcal{Q}_0 = \pm B + |B| + \alpha^{-1}\mathcal{Q}_0 \geq 0$$

and

$$\begin{aligned}\mathcal{D}^h\Psi_i^{\pm} &= \pm\mathcal{D}^h v_i + \mathcal{D}^h(|B| + \alpha^{-1}\mathcal{Q}_i)\\ &\geq \pm Q_i + r_i\alpha^{-1}\mathcal{Q}_i \geq \pm Q_i + \mathcal{Q}_i \geq 0,\end{aligned}$$

where we have used $D^-\mathcal{Q}_i \geq 0$ (as $\mathcal{Q}_i$ is a non-decreasing function). Thus, by using the maximum principle for $\mathcal{D}^h$, we get, $\Psi_i^{\pm} \geq 0$, *i.e.*

$$|v_i| \leq |B| + \alpha^{-1}\mathcal{Q}_i, \quad i = 0, \ldots, N.$$

□

Lemma 6.2.2. The solution Y of the discrete problem (6.9) satisfies

$$||Y||_{\bar{G}^N} \leq C(|B| + \|\mathcal{F}\|_{G^N}), \quad \text{where} \quad \mathcal{F}_i = f(x_i, 0) + \sum_{m=1}^{i} h_m R(x_i, x_{m-1}, 0).$$

Proof. We rewrite the discrete problem (6.9) as follows

$$\varepsilon D^- Y_i + r_i Y_i = Q_i, \quad i = 1, \ldots, N, \quad Y_0 = B$$

with

$$r_i = \frac{\partial f}{\partial y}(x_i, \tilde{Y}_i), \quad Q_i = -\mathcal{F}_i - \sum_{m=1}^{i} h_m \frac{\partial R}{\partial y}(x_i, x_{m-1}, \hat{Y}_{m-1}) Y_{m-1},$$

$$\tilde{Y}_i = \theta Y_i, \ \hat{Y}_m = \gamma Y_m, \ 0 < \theta, \gamma < 1.$$

Now

$$\begin{aligned} |Q_i| &\leq |\mathcal{F}_i| + \sum_{m=1}^{i} h_m \left| \frac{\partial R}{\partial y}(x_i, x_{m-1}, \hat{Y}_{m-1}) \right| |Y_{m-1}| \\ &\leq \|\mathcal{F}\|_{G^N} + \sum_{m=1}^{i} h_m \Lambda |Y_{m-1}|, \end{aligned}$$

where $\Lambda = \max |\frac{\partial R}{\partial y}|$. Thus, applying Lemma 6.2.1, we get

$$|Y_i| \leq |B| + \alpha^{-1} \|\mathcal{F}\|_{G^N} + \alpha^{-1} \sum_{m=1}^{i} h_m \Lambda |Y_{m-1}|.$$

So, applying the discrete analogue of Gronwall's inequality [134], we get

$$||Y||_{\bar{G}^N} \leq (|B| + \alpha^{-1} \|\mathcal{F}\|_{G^N}) e^{\alpha^{-1}\Lambda}.$$

Hence, the lemma is proved. □

6.3 Error analysis

In this section we derive a posteriori error estimate for the discrete problem (6.9). Suppose $\widetilde{Y}$ is the piecewise linear interpolant of the numerical solution $\{Y_i\}$, so that $\widetilde{Y}$ is continuous on G, linear on each $[x_{i-1}, x_i]$, and $\widetilde{Y}(x_i) = Y_i, \ 0 \leq i \leq N$. Further,

for $x \in (x_{i-1}, x_i)$, we have

$$\widetilde{Y}(x) = Y_i + (x - x_i)D^-Y_i \quad \text{and} \quad \widetilde{Y}(x) = Y_{i-1} + (x - x_{i-1})D^-Y_i.$$

Theorem 6.3.1. Suppose y is the solution of (6.1), Y is the solution of (6.9) on an arbitrary mesh $\{x_i\}$, and $\widetilde{Y}$ is its piecewise linear interpolant. Then

$$\|\widetilde{Y} - y\|_{\bar{G}} \leq C \max_{1\leq i\leq N} h_i \left\{1 + |D^-Y_i| + h_i|D^-Y_i|^2\right\}.$$

Proof. Using (6.1) we get

$$\mathcal{T}\widetilde{Y}(x) - \mathcal{T}y(x) = \varepsilon(\widetilde{Y}(x))' + f(x, \widetilde{Y}(x)) + \int_0^x R(x, s, \widetilde{Y}(s))ds.$$

Note that $(\widetilde{Y}(x))' = D^-Y_i,\ x \in (x_{i-1}, x_i), 1 \leq i \leq N$. We define auxiliary functions p and q by $p(x) := f(x, \widetilde{Y}(x))$ and $q(x, s) := R(x, s, \widetilde{Y}(s))$, respectively. Suppose $\widetilde{p}$ is the piecewise linear interpolant of p on $\bar{G}^N$. Further, suppose $\widetilde{q}$ is the piecewise linear interpolant of q in s variable on $\bar{G}^N$. Note that $p(x_i) = f(x_i, Y_i)$ and $q(x_i, x_{m-1}) = R(x_i, x_{m-1}, Y_{m-1})$. Also, for $x \in (x_{i-1}, x_i)$ and $s \in (x_{m-1}, x_m)$, we have

$$\widetilde{p}(x) = p(x_i) + (x - x_i)D^-p(x_i) \quad \text{and} \quad \widetilde{q}(x, s) = q(x, x_{m-1}) + (s - x_{m-1})D^-q(x, x_m).$$

Using these auxiliary functions and their interpolants, for $x \in (x_{i-1}, x_i)$, we have

$$\begin{aligned}
\mathcal{T}\widetilde{Y}(x) - \mathcal{T}y(x) &= \varepsilon(\widetilde{Y}(x))' + p(x) + \int_0^x q(x, s)\, ds \\
&= \varepsilon(\widetilde{Y}(x))' + \widetilde{p}(x) + (p(x) - \widetilde{p}(x)) \\
&\qquad + \int_0^x \left(\widetilde{q}(x, s) + \left(q(x, s) - \widetilde{q}(x, s)\right)\right) ds \\
&= \varepsilon D^-Y_i + \left(p(x_i) + (x - x_i)D^-p(x_i)\right) + \left(p(x) - \widetilde{p}(x)\right)
\end{aligned}$$

$$
\begin{aligned}
&+\sum_{m=1}^{i-1}\int_{x_{m-1}}^{x_m}\left[q(x,x_{m-1})+(s-x_{m-1})D^-q(x,x_m)\right]\,ds\\
&\quad+\int_{x_{i-1}}^{x}\left[q(x,x_{i-1})+(s-x_{i-1})D^-q(x,x_i)\right]\,ds+\int_0^x\Big(q(x,s)\\
&\qquad-\widetilde{q}(x,s)\Big)\,ds+\sum_{m=1}^{i}h_m q(x_i,x_{m-1})-\sum_{m=1}^{i}h_m q(x_i,x_{m-1})\\
&=(x-x_i)D^-p(x_i)+\big(p(x)-\widetilde{p}(x)\big)+\sum_{m=1}^{i}h_m\big(q(x,x_{m-1})-q(x_i,x_{m-1})\big)\\
&\quad+\sum_{m=1}^{i-1}\int_{x_{m-1}}^{x_m}(s-x_{m-1})D^-q(x,x_m)\,ds+\int_{x_{i-1}}^{x}(s-x_{i-1})D^-q(x,x_i)\,ds\\
&\quad+\int_0^x\left(q(x,s)-\widetilde{q}(x,s)\right)\,ds+(x-x_{i-1})q(x,x_{i-1}).
\end{aligned}
\tag{6.12}
$$

Now we estimate separately each of the terms in (6.12). Using the standard interpolation error estimate, for $x\in(x_{i-1},x_i)$, we have

$$
|p(x)-\widetilde{p}(x)|\le\left\{\frac{h_i^2}{8}\sup_{(x_{i-1},x_i)}|p''(x)|\right\},
$$

where

$$
p''(x)=f_{xx}(x,\widetilde{Y}(x))+2(\widetilde{Y}(x))'f_{xy}(x,\widetilde{Y}(x))+[(\widetilde{Y}(x))']^2f_{yy}(x,\widetilde{Y}(x)).
$$

Therefore, for $x\in(x_{i-1},x_i)$, we have

$$
|p(x)-\widetilde{p}(x)|\le Ch_i^2\left(1+|D^-Y_i|+|D^-Y_i|^2\right). \tag{6.13}
$$

Similarly, for $x\in(x_{i-1},x_i)$ and $s\in(x_{m-1},x_m)$, $m=1,2\ldots,i$, we have

$$
|q(x,s)-\widetilde{q}(x,s)|\le Ch_m^2\left(1+|D^-Y_m|+|D^-Y_m|^2\right).
$$

Consequently,

$$\begin{aligned}\left|\int_0^x (q(x,s)-\widetilde{q}(x,s))\,ds\right| &\le \sum_{m=1}^{i-1}\int_{x_{m-1}}^{x_m} |q(x,s)-\widetilde{q}(x,s)|\,ds \\ &\qquad + \int_{x_{i-1}}^{x} |q(x,s)-\widetilde{q}(x,s)|\,ds \\ &\le C \max_{1\le m\le i}\left\{h_m^2\left(1+|D^-Y_m|+|D^-Y_m|^2\right)\right\} \\ &\qquad \times\left(\sum_{m=1}^{i-1}\int_{x_{m-1}}^{x_m} ds + \int_{x_{i-1}}^{x} ds\right) \\ &\le C \max_{1\le m\le i}\left\{h_m^2\left(1+|D^-Y_m|+|D^-Y_m|^2\right)\right\}. \qquad (6.14)\end{aligned}$$

Also,

$$\begin{aligned}|D^-p(x_i)| &= \left|\frac{f(x_i,\widetilde{Y}(x_i))-f(x_{i-1},\widetilde{Y}(x_{i-1}))}{h_i}\right| \\ &= \left|\frac{f(x_i,\widetilde{Y}(x_i))-f(x_{i-1},\widetilde{Y}(x_i))+f(x_{i-1},\widetilde{Y}(x_i))-f(x_{i-1},\widetilde{Y}(x_{i-1}))}{h_i}\right| \\ &\le \left|\frac{\partial f}{\partial x}(\xi_i^{(1)},\widetilde{Y}(x_i))\right| + \left|\frac{\partial f}{\partial y}(x_{i-1},\sigma_i^{(1)})\right||D^-Y_i|, \qquad (6.15)\end{aligned}$$

where $\xi_i^{(1)} \in (x_{i-1},x_i)$ and $\sigma_i^{(1)} \in (\widetilde{Y}(x_{i-1}),\widetilde{Y}(x_i))$. Thus, we get

$$|D^-p(x_i)| \le C(1+|D^-Y_i|). \qquad (6.16)$$

Using similar calculations we get

$$|D^-q(x,x_m)| \le \left|\frac{\partial R}{\partial s}(x,\xi_m^{(2)},\widetilde{Y}(x_m))\right| + \left|\frac{\partial R}{\partial y}(x,x_m,\sigma_m^{(2)})\right||D^-Y_m|,$$

where $\xi_m^{(2)} \in (x_{m-1},x_m)$ and $\sigma_m^{(2)} \in (\widetilde{Y}(x_{m-1}),\widetilde{Y}(x_m))$. Thus, we get

$$|D^-q(x,x_m)| \le C(1+|D^-Y_m|). \qquad (6.17)$$

Now

$$\begin{aligned}\left|\sum_{m=1}^{i-1}\int_{x_{m-1}}^{x_m}(s-x_{m-1})D^-q(x,x_m)\,ds\right| &+ \left|\int_{x_{i-1}}^{x}(s-x_{i-1})D^-q(x,x_i)\,ds\right| \\ &\le \sum_{m=1}^{i-1} h_m|D^-q(x,x_m)|\int_{x_{m-1}}^{x_m} ds + h_i|D^-q(x,x_i)|\int_{x_{i-1}}^{x} ds \\ &\le \max_{1\le m\le i} h_m|D^-q(x,x_m)|\left(\sum_{m=1}^{i-1}\int_{x_{m-1}}^{x_m} ds + \int_{x_{i-1}}^{x} ds\right) \\ &\le C\max_{1\le m\le i} h_m(1+|D^-Y_m|), \end{aligned} \tag{6.18}$$

$$\sum_{m=1}^{i} h_m\big|q(x,x_{m-1})-q(x_i,x_{m-1}))\big| \le Ch_i \quad\text{and}\quad |(x-x_{i-1})q(x,x_{i-1})| \le Ch_i. \tag{6.19}$$

Now using all these estimates from (6.13)-(6.19) in (6.12), we obtain

$$\|\mathcal{T}\widetilde{Y}-\mathcal{T}y\|_G \le C\max_{1\le i\le N} h_i\left\{1+|D^-Y_i|+h_i|D^-Y_i|^2\right\}. \tag{6.20}$$

Hence, from Lemma 6.1.1, we get the desired a posteriori error estimate.

□

6.4 Numerical experiments

We consider the following test problem

$$\begin{cases} \varepsilon y' + y^3 + 3y + \int_0^x y^2(s)\,ds = e^{-\frac{3x}{\varepsilon}} - \frac{1}{2}\varepsilon e^{-\frac{2x}{\varepsilon}} + 2e^{-\frac{x}{\varepsilon}} + \frac{\varepsilon}{2}, \quad x\in(0,1], \\ y(0)=1. \end{cases} \tag{6.21}$$

The exact solution of the test problem is given by $y(x)=e^{-\frac{x}{\varepsilon}}$. The quasilinearization technique for nonlinear problems is a Newton like method which gives an iterative

scheme [109, 135] for the discrete problem (6.9) as follows

$$\begin{cases} Y_i^{(r)} = \frac{P_i Y_{i-1}^{(r)} - f(x_i, Y_i^{(r-1)}) - \frac{\partial f}{\partial y}(x_i, Y_i^{(r-1)}) Y_i^{(r-1)} - A_i}{P_i + \frac{\partial f}{\partial y}(x_i, Y_i^{(r-1)})}, \quad i = 1, \ldots, N, \\ Y_0^{(r)} = B, \end{cases} \tag{6.22}$$

where $Y_i^{(0)}$ is given and

$$\begin{aligned} P_i &= \varepsilon / h_i, \\ A_i &= \sum_{k=1}^{i} h_k R(x_i, x_{k-1}, Y_{k-1}^{(r)}). \end{aligned} \tag{6.23}$$

We use the condition

$$\max_i \left| Y_i^{(r)} - Y_i^{(r-1)} \right| \leq 10^{-5},$$

as the stopping criterion and $Y_i^{(0)} = 0$ as the initial iteration for the iterative scheme.

We consider adaptive mesh generation algorithm originally proposed by de Boor [136]. In literature, it has been utilized for several classes of singularly perturbed problems (see [61, 62, 107, 115, 137, 138] and the references therein). The convergence of the algorithm is studied in [71] for singularly perturbed problems and in [116] for regular boundary value problems. Starting with a uniform mesh the algorithm constructs a mesh that solves the equidistribution problem

$$h_i \psi_i = \frac{1}{N} \sum_{j=1}^{N} \psi_j h_j, \quad 1 \leq i \leq N, \tag{6.24}$$

where ψ is the monitor function. For our problem, $\psi_i = 1 + |D^- Y_i| + h_i |D^- Y_i|^2$, as suggested by Theorem 6.3.1. It was pointed out in [71] that it is not necessary to enforce (6.24) strictly. It is sufficient to stop the algorithm when the following

weakened equidistribution principle

$$h_i\psi_i \leq \frac{C_0}{N}\sum_{j=1}^{N}\psi_j h_j, \quad 1 \leq i \leq N, \tag{6.25}$$

is satisfied for some constant $C_0 > 1$.

Algorithm 5: Numerical algorithm for the adaptive mesh and adaptive solution

Input: $N \in \mathbb{N}$, $0 < \varepsilon \leq 1$ and $C_0 = 1.1$.

Output: Equidistribution mesh $\{x_i\}$ and the solution Y_i.

1. Define the initial iteration of the adaptive mesh ($k = 0$) as a uniform mesh $x_i^{(0)} = i/N,\ i = 0, \ldots, N$.
2. Calculate $Y_i^{(k)}$ solving the discrete problem (6.9) on the mesh $\{x_i^{(k)}\}$.
3. Set $h_i^{(k)} = x_i^{(k)} - x_{i-1}^{(k)}$ and evaluate the discretized monitor function $\psi_i^{(k)}$, for $i = 1, \ldots, N$. Compute $\Psi_i^{(k)} = \sum_{j=1}^{i} h_j^{(k)}\psi_j^{(k)}$.
4. Check for the stopping criterion; if $\max_{1\leq i\leq N} h_i^{(k)}\psi_i^{(k)} \leq C_0\frac{\Psi_N^{(k)}}{N}$ holds, go to Step 6, else continue with next step.
5. Set $Z_i = i\frac{\Psi_N}{N}$ for $i = 0, \ldots, N$. Generate a new mesh $\{x_i^{(k+1)}\}$ by interpolating the points (Ψ_i^k, x_i^k) and evaluating this interpolant at Z_i, $i = 0, 1, \ldots, N$. Return to Step 2 setting $k = k + 1$.
6. Take $\{x_i^{(k)}\}$ as the final adaptive mesh and $Y_i^{(k)}$ as the adaptive solution. Stop.

Now we shall apply the proposed method on the test problem (6.21) and discuss the numerical observations in the form of tables and figures. The numerical solution obtained on the adaptive mesh is compared with the exact solution for two different values of ε in Figure 6.1, which also confirms the presence of a boundary layer near $x = 0$. We compute the solutions for the set $E_\varepsilon = \{10^{-1}, 10^{-2}, ..., 10^{-7}\}$ of values of ε and using different values of the discretization parameter N. The maximum

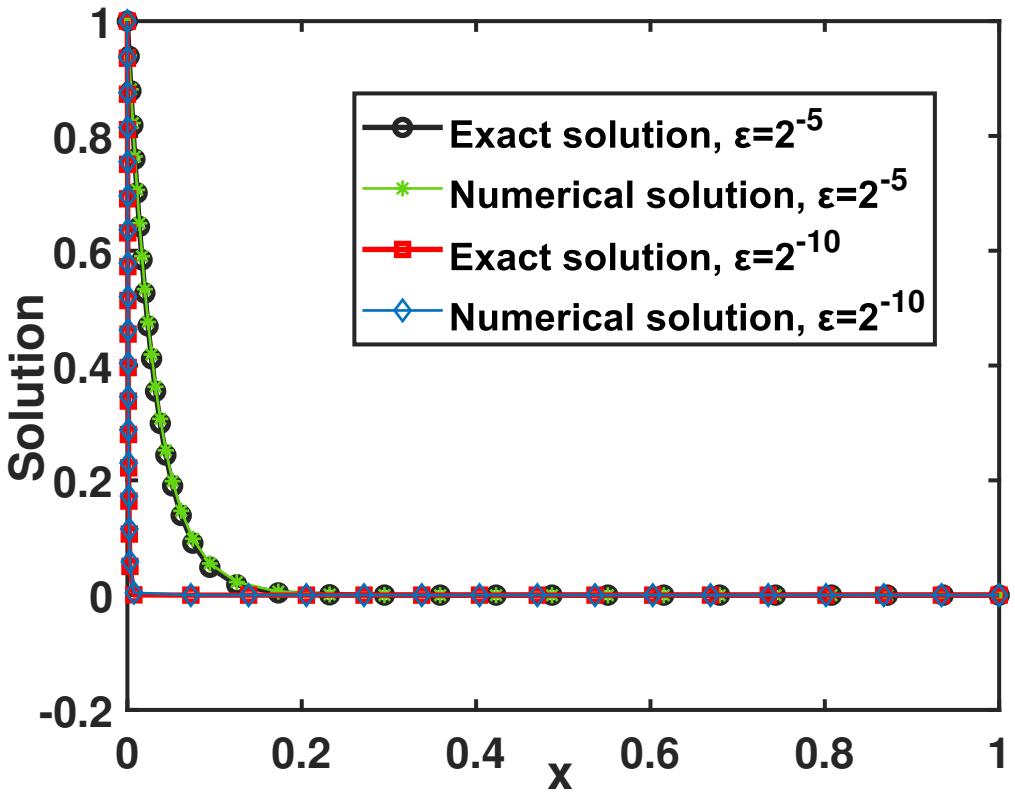

FIGURE 6.1: Comparison of the exact and numerical solutions obtained using proposed method with $N = 64$.

pointwise errors and corresponding rates of convergence are calculated by

$$E^{\varepsilon,N} = \max_{1\le i\le N} \left| Y_i^{\varepsilon,N} - y_i^{\varepsilon,N} \right|, \qquad F^{\varepsilon,N} = \log_2 \left(E^{\varepsilon,N} / E^{\varepsilon,2N} \right).$$

Parameter-robust errors and rates of convergence are computed as follows

$$E^{N} = \max_{\varepsilon} \{ E^{\varepsilon,N} \}, \qquad F^{N} = \log_2 \left(E^{N} / E^{2N} \right).$$

In Table 6.1, the results are given on the mesh generated using the proposed algorithm. Tables 6.2 and 6.3 show the results on Shishkin and Bakvalov meshes, respectively. The experimentally obtained errors and convergence rates in Table

TABLE 6.1: Errors F_ε^N and F^N, and convergence rates ϱ_ε^N and ϱ^N using the proposed method.

$\varepsilon = 10^{-r}$	$N = 32$	$N = 64$	$N = 128$	$N = 256$	$N = 512$	$N = 1024$	$N = 2048$
$r = 1$	7.6288e-03	3.8598e-03	1.9535e-03	9.8294e-04	4.9301e-04	2.4689e-04	1.2354e-04
	0.9886	0.9825	0.9909	0.9955	0.9977	0.9989	
$r = 2$	8.8662e-03	4.6227e-03	2.3514e-03	1.1873e-03	5.8714e-04	2.9690e-04	1.4924e-04
	0.9396	0.9752	0.9858	1.0159	0.9837	0.9923	
$r = 3$	9.1101e-03	4.7863e-03	2.4622e-03	1.2483e-03	6.3252e-04	3.1732e-04	1.5908e-04
	0.9285	0.9590	0.9800	0.9808	0.9952	0.9962	
$r = 4$	9.1352e-03	4.5723e-03	2.4789e-03	1.2625e-03	6.3824e-04	3.2124e-04	1.6124e-04
	0.9985	0.8832	0.9734	0.9841	0.9905	0.9944	
$r = 5$	9.1385e-03	4.8102e-03	2.3495e-03	1.2637e-03	6.3907e-04	3.2177e-04	1.6157e-04
	0.9926	1.0338	0.8947	0.9836	0.9899	0.9939	
$r = 6$	9.1381e-03	4.8110e-03	2.4804e-03	1.1964e-03	6.3916e-04	3.2182e-04	1.6161e-04
	0.9256	0.9558	1.0518	0.9045	0.9899	0.9938	
$r = 7$	9.1502e-03	4.8109e-03	2.4892e-03	1.2638e-03	6.3919e-04	3.2183e-04	1.6161e-04
	0.9275	0.9506	0.9779	0.9835	0.9899	0.9938	
F^N	9.1502e-03	4.8109e-03	2.4892e-03	1.2638e-03	6.3919e-04	3.2183e-04	1.6161e-04
ϱ^N	0.9275	0.9506	0.9779	0.9835	0.9899	0.9938	

TABLE 6.2: Errors F_ε^N and F^N, and convergence rates ϱ_ε^N and ϱ^N using Shishkin mesh.

$\varepsilon = 10^{-r}$	$N = 32$	$N = 64$	$N = 128$	$N = 256$	$N = 512$	$N = 1024$	$N = 2048$
$r = 1$	1.5734e-02	9.6739e-03	5.7331e-03	2.9809e-03	1.4979e-03	7.5086e-04	3.7591e-04
	0.7017	0.7548	0.9435	0.9928	0.9964	0.9982	
$r = 2$	1.4715e-02	9.0424e-03	5.3571e-03	3.0921e-03	1.7502e-03	9.7587e-04	5.3785e-04
	0.7025	0.7553	0.7929	0.8210	0.8428	0.8595	
$r = 3$	1.4612e-02	8.9788e-03	5.3219e-03	3.0717e-03	1.7391e-03	9.6988e-04	5.3457e-04
	0.7026	0.7546	0.7929	0.8207	0.8425	0.8594	
$r = 4$	1.4602e-02	8.9724e-03	5.3183e-03	3.0697e-03	1.7380e-03	9.6928e-04	5.3424e-04
	0.7026	0.7545	0.7929	0.8206	0.8425	0.8594	
$r = 5$	1.4601e-02	8.9718e-03	5.3180e-03	3.0694e-03	1.7379e-03	9.6922e-04	5.3421e-04
	0.7026	0.7545	0.7929	0.8206	0.8425	0.8594	
$r = 6$	1.4601e-02	8.9717e-03	5.3179e-03	3.0694e-03	1.7379e-03	9.6921e-04	5.3421e-04
	0.7026	0.7545	0.7929	0.8206	0.8425	0.8594	
$r = 7$	1.4601e-02	8.9717e-03	5.3179e-03	3.0694e-03	1.7379e-03	9.6921e-04	5.3421e-04
	0.7026	0.7545	0.7929	0.8206	0.8425	0.8594	
F^N	1.4601e-02	8.9717e-03	5.3179e-03	3.0694e-03	1.7379e-03	9.6921e-04	5.3421e-04
ϱ^N	0.7026	0.7545	0.7929	0.8206	0.8425	0.8594	

6.1 clearly confirms the optimal first order parameter-robust convergence of the proposed method. A comparison of the results is given in Table 6.4. In addition, log-log graphs of the maximum pointwise errors are plotted (in Figure 6.2) for each mesh with two different values of ε. The slopes of these plots matches with the slopes of the theoretical order plots, which again authenticates our theoretical findings. One

TABLE 6.3: Errors F_ε^N and F^N, and convergence rates ϱ_ε^N and ϱ^N using Bakhvalov mesh.

$\varepsilon = 10^{-r}$	$N = 32$	$N = 64$	$N = 128$	$N = 256$	$N = 512$	$N = 1024$	$N = 2048$
$r = 1$	9.6826e-03	5.0027e-03	2.5462e-03	1.2850e-03	6.4553e-04	3.2354e-04	1.6196e-04
	0.9527	0.9744	0.9866	0.9932	0.9966	0.9983	
$r = 2$	9.4011e-03	4.8938e-03	2.5095e-03	1.2743e-03	6.4341e-04	3.2372e-04	1.6250e-04
	0.9419	0.9636	0.9777	0.9859	0.9910	0.9943	
$r = 3$	9.3859e-03	4.8786e-03	2.4987e-03	1.2689e-03	6.4064e-04	3.2229e-04	1.6177e-04
	0.9440	0.9653	0.9775	0.9860	0.9912	0.9944	
$r = 4$	9.3838e-03	4.8770e-03	2.4973e-03	1.2684e-03	6.4035e-04	3.2214e-04	1.6170e-04
	0.9442	0.9656	0.9774	0.9861	0.9912	0.9944	
$r = 5$	9.3836e-03	4.8768e-03	2.4972e-03	1.2683e-03	6.4032e-04	3.2213e-04	1.6169e-04
	0.9442	0.9656	0.9774	0.9861	0.9912	0.9944	
$r = 6$	9.3836e-03	4.8768e-03	2.4972e-03	1.2683e-03	6.4031e-04	3.2213e-04	1.6169e-04
	0.9442	0.9656	0.9774	0.9861	0.9912	0.9944	
$r = 7$	9.3836e-03	4.8768e-03	2.4972e-03	1.2683e-03	6.4031e-04	3.2213e-04	1.6169e-04
	0.9442	0.9656	0.9774	0.9861	0.9912	0.9944	
F^N	9.3836e-03	4.8768e-03	2.4972e-03	1.2683e-03	6.4031e-04	3.2213e-04	1.6169e-04
ϱ^N	0.9442	0.9656	0.9774	0.9861	0.9912	0.9944	

TABLE 6.4: Parameter-uniform errors F^N and parameter-uniform convergence rates ϱ^N using scheme (6.9) on various meshes.

Mesh		$N = 64$	$N = 128$	$N = 256$	$N = 512$	$N = 1024$	$N = 2048$
A posteriori mesh	F^N	4.8109e-03	2.4892e-03	1.2638e-03	6.3919e-04	3.2183e-04	1.6161e-04
	ϱ^N	0.9506	0.9779	0.9835	0.9899	0.9938	
Shishkin mesh	F^N	8.9717e-03	5.3179e-03	3.0694e-03	1.7379e-03	9.6921e-04	5.3421e-04
	ϱ^N	0.7545	0.7929	0.8206	0.8425	0.8594	
Bakhvalov mesh	F^N	4.8768e-03	2.4972e-03	1.2683e-03	6.4031e-04	3.2213e-04	1.6169e-04
	ϱ^N	0.9656	0.9774	0.9861	0.9912	0.9944	

TABLE 6.5: Maximum errors F_ε^N, convergence rates ϱ_ε^N, and the number of iterations k taking $\varepsilon = 2^{-10}$ and using different values of C_0 in the algorithm.

C_0		$N = 64$	$N = 128$	$N = 256$	$N = 512$	$N = 1024$	$N = 2048$
$C_0 = 1.15$	F_ε^N	4.6827e-03	2.4396e-03	1.2467e-03	6.3188e-04	3.1696e-04	1.5153e-04
	ϱ_ε^N	0.9407	0.9685	0.9804	0.9954	1.0647	
	k	3	3	3	3	3	2
$C_0 = 1.5$	F_ε^N	4.6827e-03	2.4396e-03	1.3907e-03	5.6301e-04	2.8688e-04	1.5153e-04
	ϱ_ε^N	0.9407	0.8109	1.3046	0.9727	0.9208	
	k	3	3	2	2	2	2
$C_0 = 2.0$	F_ε^N	4.6827e-03	3.4833e-03	1.3907e-03	5.6301e-04	2.8688e-04	1.5153e-04
	ϱ_ε^N	0.4269	1.3247	1.3046	0.9727	0.9208	
	k	3	2	2	2	2	2
$C_0 = 3.0$	F_ε^N	8.5563e-03	3.4833e-03	1.3907e-03	5.6301e-04	2.8688e-04	1.5153e-04
	ϱ_ε^N	1.2965	1.3247	1.3046	0.9727	0.9208	
	k	2	2	2	2	2	2

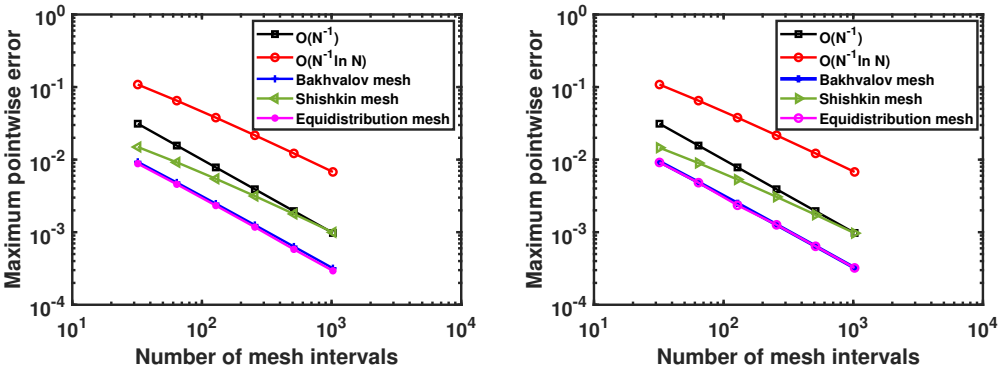

(a) For $\varepsilon = 10^{-2}$ (b) For $\varepsilon = 10^{-5}$

FIGURE 6.2: Log-log plots of maximum pointwise errors vs N for $\varepsilon = 10^{-2}$ and $\varepsilon = 10^{-5}$.

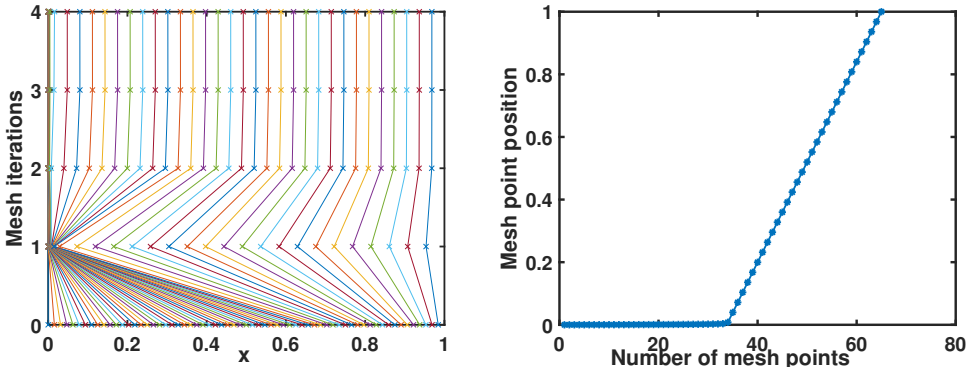

(a) Mesh trajectory (b) Mesh points position

FIGURE 6.3: Mesh trajectory and final position mesh points for $N = 64$ and $\varepsilon = 2^{-10}$.

can observe that the errors are larger for Shishkin meshes than on Bakhvalov and adaptively generated meshes, as seen with the theory as well. Further, the errors are similar on Bakhvalov meshes and adaptively generated meshes. However, the construction of Bakhvalov meshes requires a priori information about the location and width of the layers. Whereas, with the current method no a priori information is required for the solution.

To show the adaptive nature of the proposed mesh generation, in Figure 6.3, we have given the mesh trajectory as the algorithm moves with the iterations and the final mesh points position. The mesh points are condensing towards the left boundary

and finally adapts the solution behaviour by itself. This confirms the adaptivity of the generated mesh. Further, to show the influence of the value of C_0, in Table 6.5, we give the maximum pointwise errors, rates of convergence and the number of iterations the mesh generation algorithm takes before satisfying the stopping criterion for different values of C_0. From this table we can observe that as we choose the values C_0 close to 1 the number of iterations is more but the solutions are more accurate. However, we can conclude that the numerical solution converges after few iterations.

6.5 Conclusions

A nonlinear singularly perturbed VIDE is considered. The discretization of the problem is done on an arbitrary non-uniform mesh by an implicit finite difference scheme which comprises of an implicit difference operator for the derivative term and an appropriate quadrature rule for the integral term. We derived a posteriori error estimate in the maximum norm for the scheme that holds true uniformly in ε. Numerical experiments are performed and results are reported for validation of the theoretical error estimates.

****